

Molecular Motion and Phase Changes in Long Chain Solid Normal Alkanes as Studied by ^1H and ^{13}C NMR

Takahiro UEDA, Sadamu TAKEDA, Nobuo NAKAMURA,* and Hideaki CHIHARA
Department of Chemistry, Faculty of Science, Osaka University, Toyonaka, Osaka 560
(Received December 18, 1990)

Proton spin-lattice and dipolar relaxation times and ^{13}C CP/MAS NMR spectra were measured on crystalline samples of $n\text{-C}_{50}\text{H}_{102}$ and long chain normal alkanes (n -alkanes) with average molecular weight of 595, 1214, and 2305 in order to characterize the static and dynamic molecular structures in the solid state. The ^{13}C CP/MAS spectra indicate that the molecules take all-trans conformation in the orthorhombic unit cell and do not undergo any discernible change on annealing and/or quenching of specimens. On the other hand, the $T_{1\rho}$ in each material assumes a deep and clear minimum value in the orthorhombic phase; this relaxation process was unambiguously assigned to the molecular uniaxial reorientation about the long chain axis. There is a linear relation between the activation energy and the reciprocal of the chain length. In the case of $n\text{-C}_{50}\text{H}_{102}$ a solid state phase transition was found at 351 K. The $T_{1\rho}$ in the high temperature phase led to extremely high activation energy, 150 kJ mol^{-1} , which may be attributable to molecular self-diffusion or other motion accompanying drastic change in the molecular structure.

Normal alkanes, $n\text{-C}_n\text{H}_{2n+2}$, crystallize generally in an orthorhombic unit cell in which molecules assume the all-trans conformation and arrange the molecules parallel to each other.¹⁾ Short n -alkanes with carbon atoms less than 50 undergo so-called "rotational phase transition" into the high temperature phase in which molecules rotate about the long axis.²⁾ The mechanism of this kind of phase transition has been studied extensively in relation to molecular motion as well as the well-known odd-even effect.³⁾ Long-chain n -alkanes are situated between the short n -alkanes and polyethylene and possess on the one hand some common characteristics to short n -alkanes, and on the other to polyethylene. Indeed, Whiting and others⁴⁾ succeeded in the synthesis of pure long-chain n -alkanes with the number of carbons from 102 to 390 and they also found very interesting fact that the partial chain-folding occurs for the n -alkanes with the carbon number of 150 and more but not for that with 102 carbons.

Thus, the studies of structure and dynamics of long-chain n -alkanes are promising and would provide useful clue to studying variety of physical properties as well as structure of polyethylene and other complex polymers from the molecular point of view. However, although numerous thermodynamic studies have been done on high molecular weight n -alkanes,⁵⁾ there have been reported very few works on rigorous characterizations, microscopic structure, and molecular dynamical nature for these substances.

In the present work, we attempted to study long-chain n -alkanes from the molecular point of view and conducted experimental works on the phase characterization and molecular structure by differential scanning calorimetry (DSC) and solid state high resolution ^{13}C NMR and on the molecular dynamical structure by proton nuclear magnetic relaxation measurements. This paper presents the results of these experiments

and discuss the possibility of very slow molecular motion in "hard" crystalline state.

Experimental

Powdered specimens of linear polyethylene (PE) with M_w of 595, 1214, and 2305 ($M_w/M_n=1.11, 1.20, \text{ and } 1.14$, respectively) which were crystallized from *o*-dichlorobenzene solution were obtained from Scientific Polymer Products, Inc. (U.S.A.), and were used as received. Even numbered n -alkane, pentacontane ($n\text{-C}_{50}\text{H}_{102}$), was obtained from Tokyo Kasei Co. in the best commercially available quality (Purity >99%) and was also used without further purification. For proton spin-lattice relaxation time T_1 and dipolar relaxation time $T_{1\rho}$ measurements, these samples were sealed into ampoules with He exchange gas after being pumped overnight at room temperature.

All NMR measurements were carried out with a Bruker Model MSL-200 spectrometer operating at the Larmor frequencies 200.13 MHz and 50.32 MHz for proton and carbon, respectively. The proton line shape was determined by the Fourier transform of the solid echo.⁶⁾

Measurements of the proton spin-lattice relaxation time, T_1 , were made using "solid echo" method which consists of $90^\circ_x - \tau - 90^\circ_y - 90^\circ_x$ three pulse sequence.⁶⁾ Typical interval between the second and third pulses was chosen to be 10–15 μs . Measurements of the proton dipolar relaxation time, $T_{1\rho}$, were made using the three pulse Jeener-Broekaert $90^\circ_x - 45^\circ_y - \tau - 45^\circ_x$ sequence.⁷⁾ The interval between 90° and phase-shifted 45° pulses was 8–10 μs . The recovery of the magnetization in each specimen was exponential within the experimental error. The experimental errors for the T_1 and $T_{1\rho}$ were estimated to be within 5% and 10%, respectively.

^{13}C CP/MAS NMR spectra were recorded with the spectrometer described above. The applied cross-polarization time was 1 ms followed by the ^{13}C detection period during which the proton decoupling field was maintained. MAS (magic angle spinning) was carried out at a rate of 1.5–3 kHz with a double bearing type rotor made of zirconia whose volume was about 0.7 cm^3 . In the present work, the

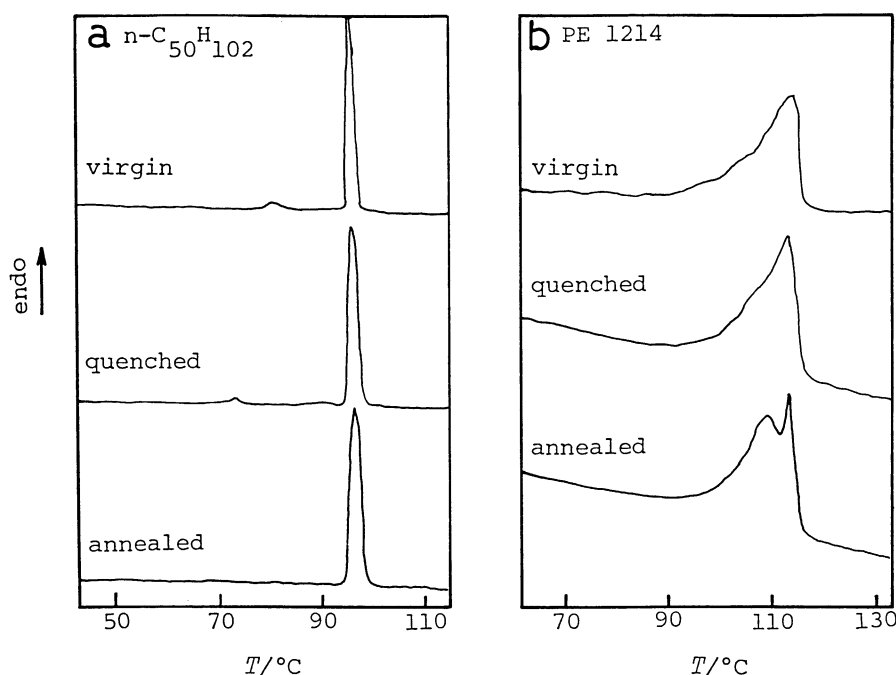


Fig. 1. Differential calorimetric scans for virgin (recrystallized from solution), quenched from the melt, and annealed specimens of $n\text{-C}_{50}\text{H}_{102}$ (a) and PE 1214 (b).

^{13}C chemical shifts relative to TMS were determined from the CO line (176.46 ppm) of solid glycine.

For all experiments, the temperature control was achieved by Bruker variable temperature unit VT-1000. The melting points and solid state phase transition points of all samples were determined by means of Shimadzu DT-30B differential scanning calorimeter with a heating rate of 5 K min^{-1} . X-Ray diffraction powder patterns were measured by means of RAD-RC type, fully automatic, X-ray diffractometer (Rigaku electronics Inc.).

Results and Discussion

X-ray diffraction powder patterns of all the specimens consisted of sharp reflections which can be indexed to the orthorhombic unit cell corresponding to ordinary polyethylene crystal and weak halo components were discerned, indicating that each specimen can be regarded as good crystals with negligible amount of amorphous components.

Melting points, probable transition points determined by DSC measurements, and crystallinity estimated by proton line shape analysis are listed in Table 1; DSC curves for $n\text{-C}_{50}\text{H}_{102}$ and PE 1214 are shown in Fig. 1(a) and (b) as typical examples.

The virgin and quenched[#] samples of $n\text{-C}_{50}\text{H}_{102}$ undergo solid state phase transition just below the melting point, while the annealed[#] sample gives no evidence of phase transition. The melting of PE 1214

Table 1. The Melting Points, the Phase Transition Points Determined by DSC, and Crystallinity for the n -Alkane Specimens with Different Thermal Histories

Sample	Treatment	Melting point/K	Transition point/K	Crystallinity
				%
$n\text{-C}_{50}\text{H}_{102}$	Virgin	366	351 ^{a)}	
	Annealed	366	—	
	Quenched	366	343, 361 ^{a)}	
PE 595	Virgin	—		
	Annealed	330		91
	Quenched	330		
PE 1214	Virgin	376		
	Annealed	380	369 ^{b)}	95
	Quenched	376	368 ^{b)}	
PE 2305	Virgin	391		
	Annealed	392	386 ^{b)}	98
	Quenched	393	386 ^{b)}	

a) Rotational phase transition for n -alkane. b) Peak or shoulder of the melting curve which was assigned to the premelting of the amorphous part.

begins near 363 K as shown in Fig. 1(b) due probably to the melting of the amorphous part, suggesting that even negligible amount of amorphous part causes premelting phenomenon in long chain alkane.⁸⁾ The proton spectrum in each substance consists of a narrow and a broad components due obviously to an amorphous part and the rigid crystalline part, respectively, in the specimen. Two components were approximated by a narrow Lorentzian peak and the

[#] Virgin sample was obtained by crystallization from solvent, quenched one by rapid solidification of the melt, and annealed one by slow cooling of the melt.

Pake doublet with an appreciable line broadening (Gaussian) and the whole spectrum was simulated by changing the composition. The result led directly to the crystallinity listed in Table 1. In the case of $n\text{-C}_{50}\text{H}_{102}$ no narrow component was observed, indicating that the material is pure crystal.

Carbon-13 CP/MAS NMR Spectra. Fig. 2(a) shows the ^{13}C CP/MAS NMR spectrum of $n\text{-C}_{50}\text{H}_{102}$ at room temperature. The spectrum of $n\text{-C}_{50}\text{H}_{102}$ consists of four sharp peaks which can be assigned according to Van der Hart⁹⁾ to, from the high field side downward, the methyl carbon, the α -methylene carbon bonded to the methyl carbon, inner carbons with trans zig-zag conformation, and the β -methylene carbon bonded to α -carbon, respectively. The signal with star is the spinning side band of the strongest signal due to inner carbons.

The facts that the inner carbon line is very sharp and located at a lower field than α -methylene peak by 8 ppm show obviously that the linear chain molecules have the all-trans conformation in the orthorhombic unit cell,⁹⁾ and moreover, the specimen contains only

negligible amounts of amorphous part. The spectrum of PE 1214 shown in Fig. 2(b) consists also of four peaks the location of which are almost the same as in $n\text{-C}_{50}\text{H}_{102}$. The line width of each peak is about twice as large as in $n\text{-C}_{50}\text{H}_{102}$ due probably to a slight disorder in the molecular arrangement associated with the molecular weight distribution. Then, the spectrum of this material shows that the molecules take the all-trans conformation. The fraction of the gauche form,¹⁰⁾ if any, is estimated to be less than 1% and that of amorphous part is negligibly small as shown in Table 1. We did not see any change in the spectrum due to quenching and/or annealing of specimen.

As to the temperature dependence of the spectra only a slight narrowing of the methyl carbon signal on heating were observed for both quenched and annealed specimens due probably to the rapid rotation of the methyl group. The α -methylene and the inner carbon line widths did not show any significant temperature dependence.

Other substances, PE 595 and PE 2305, gave similar spectra to that of PE 1214 although the line width increases slightly with the chain length. It is therefore concluded that all the materials examined here have extremely high crystallinity (see in Table 1) and the molecules assume all-trans conformation; there is no evidence of wrong, gauche conformation nor chain-folding.¹⁰⁾

Proton Spin Lattice and Dipolar Relaxation Times. n -Alkanes or linear polyethylenes consist of long $-\text{CH}_2-$ chain and terminal CH_3 groups. These different groups contribute to the proton relaxation in a different manner from each other. Therefore, the experimental relaxation rates due to these two groups under the condition that the spin temperature is established over the whole spin system, are given by

$$\frac{1}{T_1} = \frac{1}{n} \left(\frac{n(\text{CH}_2)}{T_1(\text{CH}_2)} + \frac{n(\text{CH}_3)}{T_1(\text{CH}_3)} \right), \quad (1)$$

and

$$\frac{1}{T_{1d}} = \frac{1}{n} \left(\frac{n(\text{CH}_2)}{T_{1d}(\text{CH}_2)} + \frac{n(\text{CH}_3)}{T_{1d}(\text{CH}_3)} \right), \quad (2)$$

where n is the total number of protons in the specimen and $n(\text{CH}_2)$ and $n(\text{CH}_3)$ are those in the methylene and methyl groups, respectively. In the present specimens the condition that $n(\text{CH}_2) \gg n(\text{CH}_3)$ holds and moreover, both $T_1(\text{CH}_3)$ and $T_{1d}(\text{CH}_3)$ are very long because of very rapid internal rotation of CH_3 groups. Hence we can ignore the second terms of Eqs. 1 and 2, and so the relaxation rates can be interpreted in terms of the dipolar relaxation due to the motion of the methylene groups. In such a case the relaxation process is described by a single correlation time τ_c of the motion of CH_2 segments and, under the "weak collision limit",¹¹⁾ T_1 and T_{1d} are given by

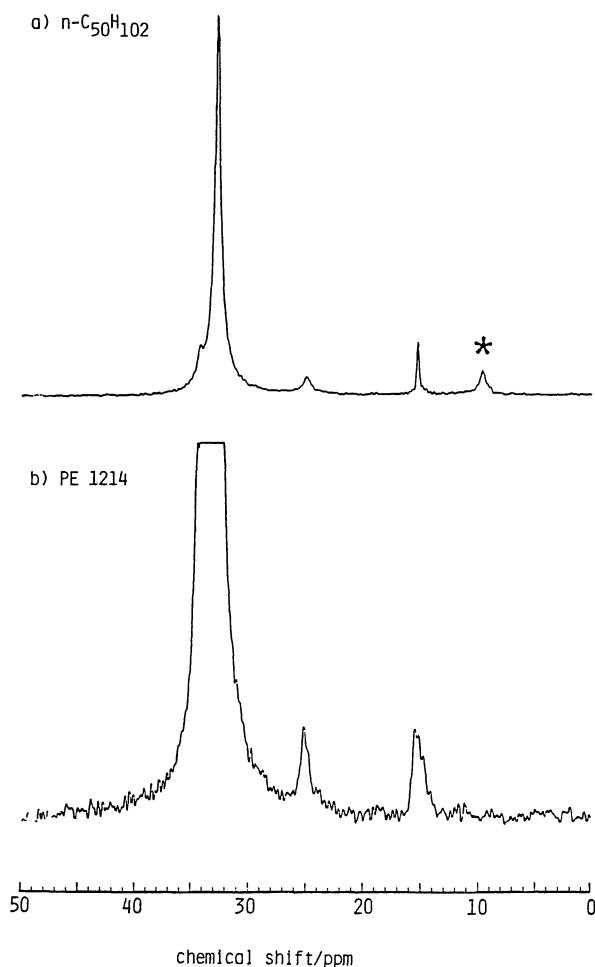


Fig. 2. ^{13}C CP/MAS NMR spectra of $n\text{-C}_{50}\text{H}_{102}$ (a) and PE 1214 (b) at room temperature. The sign (*) is the spinning side band.

$$\frac{1}{T_1} = K \left[\frac{\tau_c}{1 + \omega_0^2 \tau_c^2} + \frac{4\tau_c}{1 + 4\omega_d^2 \tau_c^2} \right], \quad (3)$$

and

$$\frac{1}{T_{1d}} = \frac{K}{2} \left[\frac{5\tau_c}{1 + \omega_0^2 \tau_c^2} + \frac{2\tau_c}{1 + 4\omega_0^2 \tau_c^2} + \frac{3\tau_c}{1 + 4\omega_d^2 \tau_c^2} \right], \quad (4)$$

where K represents the strength of the dipolar interaction; in the case of a two-spin system such as CH_2 segment $K \sim (9/40) \gamma^4 \hbar^2 / r^6$ where r is the distance between two protons and γ the proton gyromagnetic ratio, ω_0 is the Larmor frequency and $\omega_d \sim K^{1/2}$ the local field in the frequency unit. When the chain undergoes reorientation about its long axis, the intramolecular interaction between CH_2 segment brings about

$\omega_d / 2\pi \sim 1.3 \times 10^4 \text{ Hz}$. If the motion is limited to some local motion such as conformational change or kink diffusion,¹²⁾ ω_d should be much smaller.

Figure 3 shows the temperature dependence of T_1 and T_{1d} for PE 1214 between room temperature and the melting point. It shows that each of T_1 and T_{1d} for the virgin sample measured in the heating direction coincides with the result which was observed on cooling from the melt. The fact that T_1 does not vary appreciably with temperature suggests that a trace of some paramagnetic impurity governs the Zeeman spin lattice relaxation. The T_1 in PE 595 and PE 2305 behaves similarly. On the other hand, T_{1d} varies

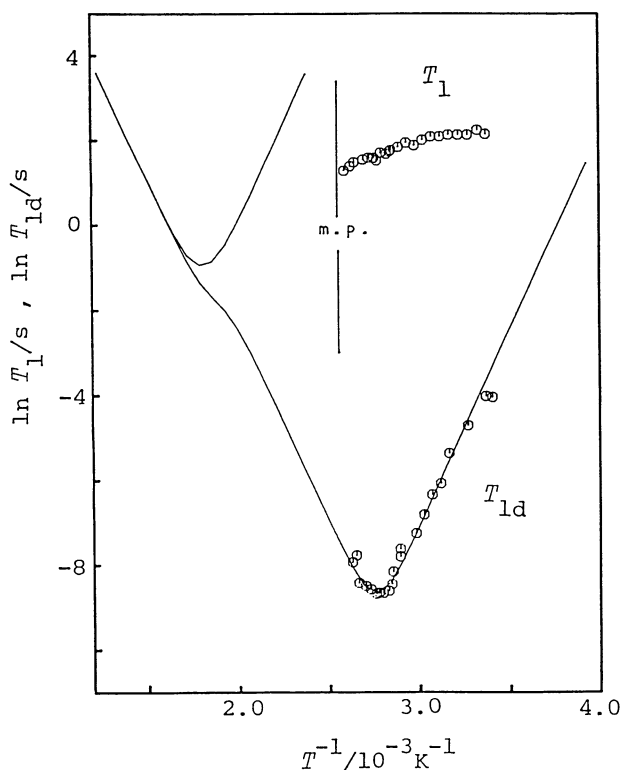


Fig. 3. Temperature dependence of proton spin lattice relaxation time (T_1) and dipolar relaxation time (T_{1d}) in PE 1214 at 200 MHz. The solid lines indicate the calculated T_1 and T_{1d} with Eqs. 4 and 5 and with the parameters listed in Table 2.

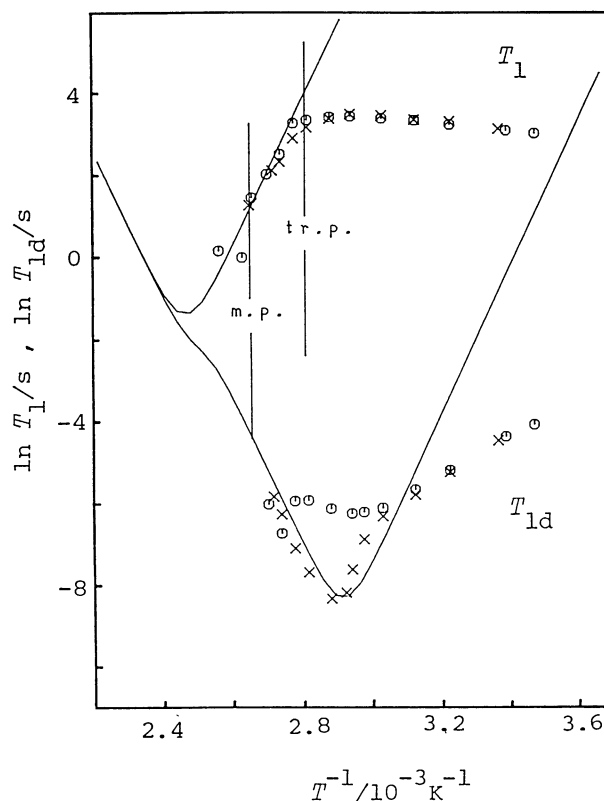


Fig. 4. Temperature dependence of proton spin lattice relaxation time (T_1) and dipolar relaxation time (T_{1d}) in $n\text{-C}_{50}\text{H}_{102}$ at 200 MHz; heating (\circ), cooling (\times). The solid lines indicate the calculated T_1 and T_{1d} with Eqs. 4 and 5 and with the parameters listed in Table 2.

Table 2. The Temperature of T_{1d} Minimum, the Activation Parameters, and Strength of the Dipolar Field for Each Substance

Sample	T_{\min}/K	$E_a/\text{kJ mol}^{-1}$	τ_0/s	K/s^{-2}	$(\omega_d/2\pi)\text{kHz}$
$n\text{-C}_{50}\text{H}_{102}$	340	42.0	2.3×10^{-12}	1.1×10^8	13
	344	150	2.3×10^{-29}	3.5×10^9	51
PE 595	286	31.0	7×10^{-12}	8.6×10^8	29
PE 1214	360	77.0	2.6×10^{-17}	2.3×10^9	23
PE 2305	365	85.0	2.4×10^{-18}	1.25×10^9	23

with temperature as expected from the usual BPP theory, Eq. 4, and assumes a minimum value at the temperature as listed in Table 2. Hence Eq. 4 was attempted to fit the experimental data in Fig. 3 assuming the Arrhenius activation process,

$$\tau_c = \tau_0 \exp(E_a/RT), \quad (5)$$

for molecular motion, and the resulting values together with those for PE 595 and PE 2305 are recorded in Table 2.

In the case of $n\text{-C}_{50}\text{H}_{102}$ the T_1 and the T_{1d} show novel temperature dependence as shown in Fig. 4. The T_1 does not change appreciably on heating up to the transition at 351 K but decreases very sharply above the transition point. This behavior of T_1 was reproduced in the cooling direction. On the other hand the T_{1d} decreases on heating and assumes a minimum value, 20 ms, at 340 K, then increases as the transition point is reached, where a sudden decrease of T_{1d} occurs. However, on cooling from the high temperature phase T_{1d} decreases remarkably, assumes a deep minimum value of 270 μs at 344 K, then increases dramatically on further cooling down to 328 K. Below 328 K the value of T_{1d} settles into that determined in the heating direction. The peculiar behavior of T_{1d} on cooling can be accounted for by reference to the results of DSC on this compound: The high temperature phase (HTP) can be easily super-cooled. In our NMR experiment it remains down to about 344 K on cooling and so the T_{1d} measured between the melting point and 344 K is attributed to that in the HTP. Between 344 K and about 333 K the phase transition to the low temperature phase (LTP) sets in so that the apparent T_{1d} in this temperature

region is the weighted average of the T_{1d} of the HTP and LTP. Since the T_{1d} in the HTP in this temperature range is very short but that in the LTP is significantly longer, the measured T_{1d} goes up dramatically as the phase transformation proceeds from the HTP to the LTP.

For the sake of data analysis, T_{1d} measured on heating was used for the molecular motion in the LTP, and T_{1d} measured between the melting point and 344 K on cooling was used for the HTP. For the LTP the value of ω_d can be accounted for by the model that all CH_2 segments are undergoing the rotation or reorientation about the long chain axis simultaneously. The results of the analysis by the above mentioned procedure are listed in Table 2. The activation energy, 42 kJ mol^{-1} , obtained here for the LTP may be compared with a value of 40 kJ mol^{-1} which was calculated for infinite chain model at 400 K by means of molecular dynamics simulation by Ryckaert and Klein.¹³⁾

On the other hand, very large values of E_a and ω_d in the HTP cannot be fitted to the uniaxial reorientation model. Generally, short n -alkanes with carbon number smaller than 44 undergo "rotational transition" in which the molecular rotation about its long axis is excited in the high temperature rotational phase.¹²⁾ In the case of $n\text{-C}_{50}\text{H}_{102}$ it is suggested that the molecular reorientation or rotation is excited to some extent in the HTP as in other shorter n -alkanes; however, as mentioned above such a local molecular motion cannot account for the extremely large E_a and ω_d . It is therefore considered that some other motion such as molecular translational self-diffusion or drastic and dynamic change of molecular shape occurs

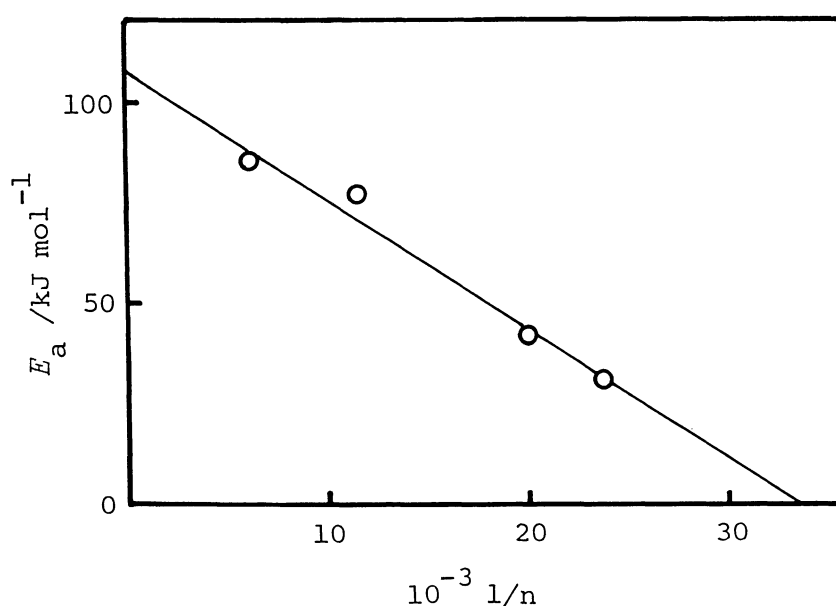


Fig. 5. The plot of E_a against the reciprocal of the number of carbons ($1/n$) in the single molecular chain.

above the transition point.¹⁴⁾

Figure 5 plots the activation energy E_a for the chain reorientation against the reciprocal of the number of carbons in the single molecular chain. This plot gives a straight line, suggesting that the E_a is not proportional to the number of CH_2 segments but instead approaches a limiting value, 100–110 kJ mol⁻¹, as n increases. This tendency of E_a resembles the chain length dependence of the melting point of long n -alkanes^{1–3)} that the melting point approaches a limiting value, about 410 K, as n increases. These facts seem to indicate that there exists some close correlation between the activation process of molecular rotation or reorientation about the long axis and the melting phenomenon.

The activation process in the low molecular weight n -alkanes cannot be predicted from Fig. 5 because the assumption of the straight line in this figure leads to the zero activation energy at $n \approx 30$; this means that the orthorhombic structure is not stable for $n < 30$. However odd-numbered n -alkanes with 9 carbons or more crystallize in the orthorhombic unit cell actually.¹⁾ We need the activation energy for short n -alkanes in order to discuss this point in greater detail but only few E_a data have been reported so far¹⁴⁾ for which some ambiguity about the assignment of the relaxation data remains.

The present work was partially supported by Grand-in-Aid for Scientific Research No. 61430006 from the Ministry of Education, Science and Culture. We are also grateful to Asahi Chemical Industry Co., Ltd. for partial financial support.

References

- 1) For example: a) A. Müller, *Proc. R. Soc. London, Ser. A*, **127**, 417 (1930); b) A. Müller and K. Lonsdale, *Acta Crystallogr.*, **1**, 129 (1948); c) M. G. Broadhurst, *J. Res. Natl. Bur. Stand., Sect. A*, **66**, 241 (1962).
- 2) a) J. Doucet, I. Denicolo, A. Craievich, and A. Collet, *J. Chem. Phys.*, **75**, 5125 (1981); b) G. Ungar, *J. Phys. Chem.*, **87**, 689 (1983).
- 3) N. G. Parsonage and L. A. K. Staveley, "Disorder in Crystals," Oxford University Press, Oxford (1978).
- 4) G. Ungar, J. Stejny, A. Keller, I. C. Bidd, and M. C. Whiting, *Science*, **229**, 386 (1985).
- 5) a) G. M. Stack, L. Mandelkern, C. Kröhnke, and G. Wegner, *Macromolecules*, **22**, 4351 (1989); b) J. D. Hoffman, *Polym. Commun.*, **27**, 39 (1986).
- 6) J. G. Powles and J. H. Strange, *Proc. Phys. Soc., London*, **82**, 6 (1963).
- 7) J. Jeener and P. Broekaert, *Phys. Rev.*, **157**, 232 (1967).
- 8) a) Y. Kim, H. L. Strauss, and R. G. Snyder, *J. Phys. Chem.*, **93**, 485 (1989); b) **93**, 7520 (1989).
- 9) D. L. Van der Hart, *J. Magn. Reson.*, **44**, 117 (1981).
- 10) I. Ando, T. Yamanobe, T. Sorita, T. Komoto, H. Sato, K. Deguchi, and M. Imanari, *Macromolecules*, **17**, 1955 (1984).
- 11) R. Van Steenwinkel, *Z. Naturforsch. A*, **24**, 1526 (1969).
- 12) a) W. Pechhold, *Kolloid Z. u. Z. Polym.*, **228**, 1 (1968); b) R. Kimmich, *Colloid Polym. Sci.*, **252**, 786 (1974).
- 13) J.-P. Ryckaert and M. L. Klein, *J. Chem. Phys.*, **85**, 1613 (1986).
- 14) M. Stohrer and F. Noack, *J. Chem. Phys.*, **67**, 3729 (1977).